The Performance of Alloyed (CdS$_{0.33}$Se$_{0.67}$) Quantum Dots –Sensitized TiO$_2$ solar cell

S. Abdallah[1, 2]

[1]Department of Mathematical and Physical Engineering, Faculty of Engineering (Shoubra) Benha University, Cairo, Egypt.
[2]Department of Physics, Faculty of Science, Taif University, Taif, Saudi Arabia.

The performance of alloyed CdS$_{0.33}$Se$_{067}$ quantum dots sensitized solar cells (QDSSCs) is studied. Fluorine doped Tin Oxide (FTO) substrates were coated with 20 nm-diameter TiO$_2$ nanoparticles (NPs). Presynthesized CdS$_{0.33}$Se$_{067}$ quantum dots (QDs) of radius 3.1 nm, were deposited onto TiO$_2$ nanoparticles (NPs) using direct adsorption (DA) method, by dipping for different times at ambient conditions. The FTO counter electrodes were coated with platinum, while the electrolyte containing I$^-$/I$_3^-$ redox species was sandwiched between the two electrodes. The characteristic parameters of the assembled QDSSCs were measured under AM 1.5 sun illuminations. The current density- voltage (J-V) characteristic curves of the assembled cells were of different dipping times. The maximum values of short circuit current density (J$_{sc}$) and conversion efficiency (η) are 1.115 mA/cm^2 and 0.25% respectively, corresponding to 6 h dipping time. Furthermore, the J$_{sc}$ increases linearly with increasing the intensities of the sun light which indicates the linear response of the assembled cells.

1. Introduction:

Recently, quantum dot-sensitized solar cells (QDSSCs) have been considered as a possible alternative to dye-sensitized solar cells (DSSCs), [1] because semiconductor quantum dots (QDs) exhibit outstanding properties such as a high extinction coefficient, efficient charge separation, spectral tunability by particle size, and multiple exciton generation [2]. In the case of QDSSCs, excited electrons of semiconductor nanocrystals are injected into a large band gap semiconductor such as TiO$_2$ [3-8] or ZnO [8-12], while holes are scavenged by a redox couple. However, the tuning of electronic, optical, and magnetic properties by changing the particle size may cause problems in some applications. To overcome these problems, a new class of alloyed semiconductor QDs has been studied, because these alloyed QDs provide a way for continuous tuning of quantum confinement and hence the effective band gap without changing the particle size. The band gap of CdS$_x$Se$_{1-x}$ alloyed QDs can be adjusted by varying

the sulfur concentration [13], spanning the compositional range from pure CdSe(x=0) to pure CdS(x=1), where the band gap energies ranges from the UV to the visible. This makes CdS_xSe_{1-x} a potentially favorable material as a sensitizer for quantum dots sensitized solar cells (QDSSCs). There are many variables to be studied and improved such as synthetic routes for the QDs and the capping agent material used. In addition, the adsorption techniques used to anchor these QDs onto the large band gap metal oxides. Some of these adsorption methods: (i) in situ growth of QDs by either CBD technique, containing both the cationic and anionic precursors [3, 12, 14-16] or successive ionic layer adsorption and reaction (SILAR) deposition method [6, 9, 17-19], (ii) deposition of presynthesized colloidal QDs by either direct adsorption (DA) for different dipping times [5, 20, 21], or by linker-assisted adsorption (LA) [18, 21-23]. and (iii) electrophoretic deposition (EPD) method [22, 24].

In this work, we prepared the alloyed composite $CdS_{0.33}Se_{067}$ using chemical deposition (CD) technique to be used as a sensitizer in QDSSCs. These colloidal QDs were adsorbed onto TiO_2 NPs by DA technique for different dipping times under ambient conditions. The $CdS_{0.33}Se_{067}$ QDSSCs characteristic parameters (short circuit current density (J_{sc}), open circuit voltage (V_{oc}), fill factor (FF), and efficiency for energy conversion (η) were measured.

2. Experiment:

2.1. Synthesis of $CdS_{0.33}Se_{0.67}$ quantum dots

An alloy $CdS_{0.33}Se_{067}$ nanocrystals was prepared by the method of Talapin et al [25] by varying the amount of the second precursor (S). Cadmium solution was prepared by adding CdO to a stearic acid, and heated up to 170 ^{o}C till the red color of CdO disappears to ensure that the reaction between CdO and stearic acid is complete and CdO completely transform to Cd sterate. (TOPO) and (HDA) are added to the reaction mixture and heated at 200 ^{o}C. Sulphur solution was prepared by mixing sulphur in (TOP). Selenium solution was also prepared by dissolving selenium in (TOP). Appropriate amounts of sulphur and selenium solutions were mixed together to give the above ratios. The mixture was then injected into the cadmium solution at a temperature 200 °C. Small volumes of sample were taken and quenched in toluene 25 °C to terminate the growth of the particle immediately. The resulting alloyed nanocrystal in toluene solution were precipitated out by using ethanol and isolated by centrifugation and decantation.

2.2. Preparation of solar cell electrodes

The TiO_2 colloidal paste was prepared by the method of G. Syrrokostas et al [26]. Three grams of commercial TiO_2 nanopowder (20 nm) (Degussa P-25 Titanium dioxide consists of 80% anatase and 20% rutile) was ground in a porcelain mortar and mixed with a small amount of distilled water (1 ml) containing acetyl acetone (10% v/v) to create the paste. Acetyl acetone was used as a dispersing agent, since it prevents coagulation of TiO_2 nanoparticles and affects the porosity of the film. The paste was diluted further by slow addition of distilled water (4 ml) under continued grinding. The addition of water controls the viscosity and the final concentration of the paste. Finally, a few drops of a detergent (Triton X-100) were added to facilitate the spreading of the paste on the substrate, since this substance has the ability to reduce surface tension, resulting in even spreading and reducing the formation of cracks. The TiO_2 paste was deposited on a conducting glass substrate of SnO_2:F with sheet resistance of 7 Ω/sq and >80% transmittance in the visible region, using a simple doctor blade technique. This was followed by annealing at $450^{\circ}C$ for 30 min and the final thickness was 8μm after the solvent evaporation. Then the TiO_2 films were dipped into a colloidal solution of presynthesized $CdS_{0.33}Se_{067}$ QDs to form four working electrodes. The counter electrodes were prepared by coating another FTO substrate sheet of resistance of 7 Ω/sq with Pt.

2.3. Assembly of QDSSC:

The alloyed $CdS_{0.33}Se_{067}$ QDs sensitized TiO_2 electrode and the Pt counter electrode were assembled as a sandwich type cell using clamps. Both electrodes were sealed using a hot-melt polymer sheet (solaronix, SX1170-25PF) of 25 μm thickness in order to avoid evaporation of electrolyte. Finally, Iodide electrolyte solution was prepared by dissolving 0.127 g of 0.05 M Iodine (I_2) in 10 mL of water-free ethylene glycol, then adding 0.83 g of 0.5 M potassium iodide (KI). The electrolyte was inserted in the cell with a syringe, filling the space between the two electrodes.

2.4. Measurements:

The sizes of the QDs were measured by transmission electron microscope (TEM). The absorption spectra of the alloyed $CdS_{0.33}Se_{067}$ QDs (before and after adsorption on TiO_2 electrodes) were recorded using a UV–Visible spectrophotometer (JASCO V-670). The current density–voltage (J–V) characteristics were recorded with a Keithley 2400 voltage source/ammeter using GreenMountain IV-Sat 3.1 software, when the $CdS_{0.33}Se_{067}$ QDSSCs were subjected to the irradiation of a solar simulator (ABET technologies**,** Sun 2000 Solar Simulators, USA) operating at 100 mW/cm^2 (AM1.5G). The intensity of the incident solar illumination was adjusted to 1 sun condition using a Leybold certified silicon reference solar cell (Model: [57863] Solar cell 2 V/0.3 A STE 4

/100). A J-V characteristic curve of all four sizes of CdTe QDSSC (for 50 hours dipping time) were studied at various illumination intensities using attenuators and calibrated by the previous Si reference solar cell. All experiments were carried out under ambient conditions.

3. Results and Discussion:-

3.1. Characterization of the alloyed CdS$_{0.33}$Se$_{067}$ QDs:

The average particle size of all prepared alloyed CdS$_{0.33}$Se$_{067}$ QDs was estimated using transmission electron microscope (TEM). Which is approximately 3 nm. Fig. 1(a), show the TEM micrographs of CdS$_{0.33}$Se$_{067}$.
The optical absorption spectrum of the samples in colloidal solution was obtained by regular UV-Vis. absorption and is given in Fig. 1(b). It is easily observed that there is excitonic absorption edges at 557 nm. The corresponding QDs radius was calculated by the effective mass approximation (EMA) model [27-30] given by:

$$E_{g(nano)} = E_{g(bulk)} + \frac{h^2}{8R^2}\left(\frac{1}{m_e} + \frac{1}{m_h}\right) - \frac{1.8e^2}{4\pi\varepsilon\varepsilon_0 R} - small \quad terms \qquad (1)$$

where $E_{g(bulk)}$ is the bulk CdS$_{0.33}$Se$_{067}$ band gap energy value, $E_{g(nano)}$ is the nano crystal band gap, R is the radius, and $m_{e,h}$ is the reduced mass of the electron and the hole, ε_0 is the permittivity of vacuum and ε is the relative dielectric constant for CdS$_{0.33}$Se$_{067}$. In order to calculate the band gap for the alloyed nanocrystals semiconductor, we first employed Vegard's law [31] to calculate the band gap of bulk semiconductor alloy, effective mass, and the dielectric constant ε, then, we use the EMA model to get the band gap of the alloyed QDs. For bulk alloyed material, Vegard's law gives the following relation for the parameters of the composition [31].

$$\square \ (CdS_xSe_{1-x}) = x \ \square \ (CdS) + (1-x) \ \square \ (CdSe) - x(1-x)b \qquad (2)$$

Where $\square$ stands for E$_g$ (bulk band gap for CdSe (=1.74 eV [27, 32]) and for CdS (=2.42 eV [32]), m (bulk effective mass), ε (bulk dielectric), and b is the bowing parameter = 0.3 [31]. In order to obtain the EMA parameters for the alloyed QDs, Vegard's law was applied to each parameter; the band gap E$_g$ (bulk), effective mass, and the dielectric. Given that the values of ε, m_h, and m_e, for CdS (5.29 , 0.7 m$_o$ and 0.2 m$_o$) and for CdSe (5.8, 0.4 m$_o$ and 0.13m$_o$) [32], the particle size was calculated as 3.1 nm which is comparable to that obtained by TEM image.

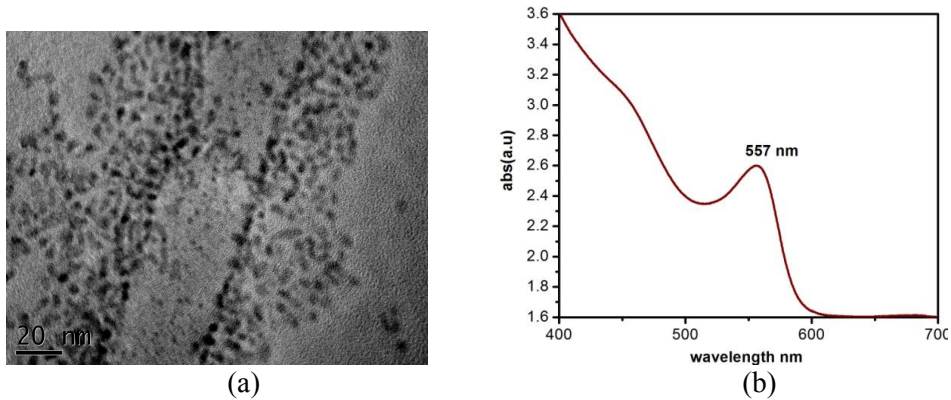(a)   (b)

Fig. (1) a): TEM micrograph for $CdS_{0.33}Se_{067}$ and (b) UV-Vis absorption spectra

Figure (2) shows the absorption spectra of the working electrode for different dipping times as indicated. It is clear that the absorption increase with the increase of DA dipping times, indicating an increase of the adsorbed amount of $CdS_{0.33}Se_{067}$. Furthermore, it is seen that the adsorption amount of $CdS_{0.33}Se_{067}$ increase until 24 h dipping time; with no farther increase for longer dipping time. Therefore it is observed that the maximum penetration and wetting of the QDs solution in the nonoporous TiO_2 matrix occurs at this time.
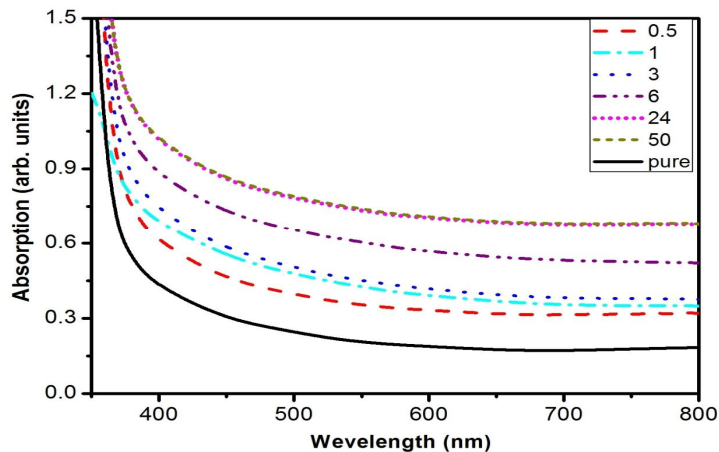

Fig. (2): UV– Vis. Absorption spectra of $CdS_{0.33}Se_{067}$ deposited on TiO_2 NPs at 0 ,0.5 1, 3 , 6 , 24 and 50 hours dipping times

To ensure, that the adsorption of CdS_xSe_{1-x} QDs onto the TiO_2 electrode takes place, EDX was performed. The EDX for a TiO_2 electrode and a $CdS_{0.33}Se_{067}$ QDs/ TiO_2 electrode are shown in Fig (3 a and b) respectively. It is easily observed that, Cd, S, and Se, which do not appear in the EDX of the TiO_2 electrode, appear in the EDX of $CdS_{0.33}Se_{067}$ QDs / TiO_2
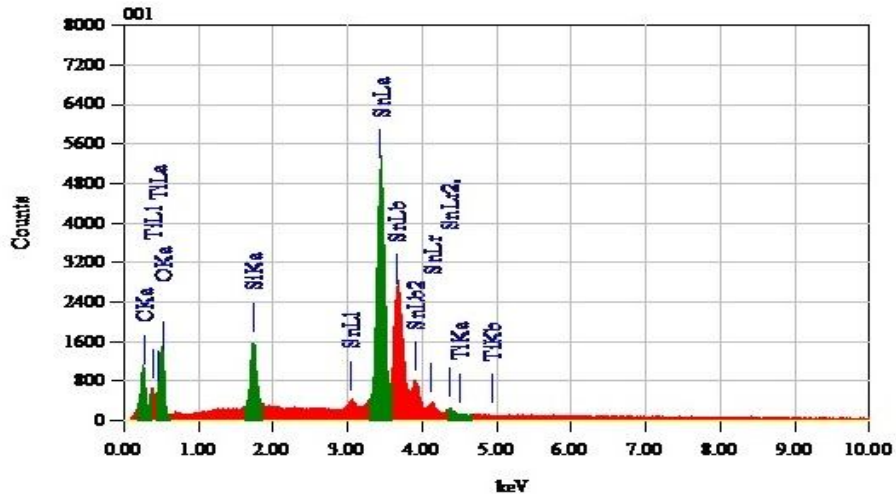
(a)
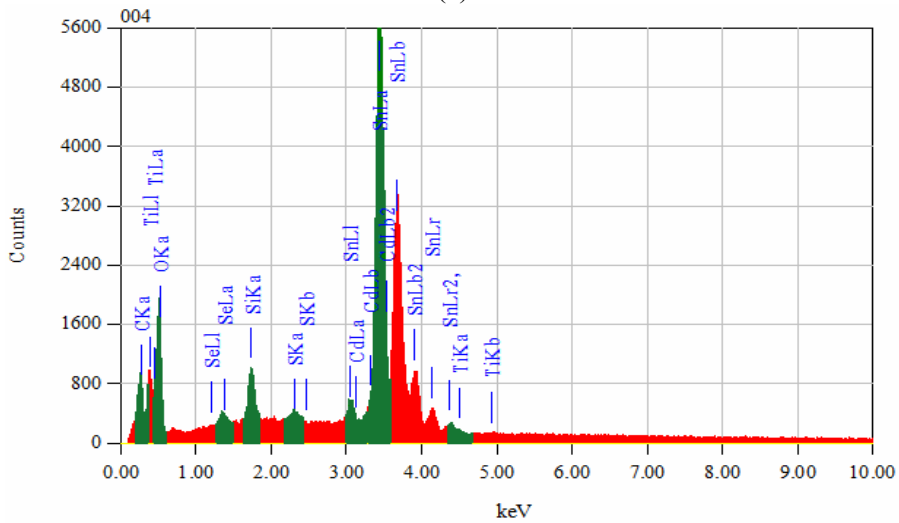
(b)

Fig. (3): EDX data: (a) nanocrystalline TiO_2 film on FTO, and (b) $CdS_{0.33}Se_{067}$ quantum dots adsorbed on a TiO_2 film

The J-V characteristics of the assembled $CdS_{0.33}Se_{067}$ QDSSCs for different deposition times (0.5, 1, 6, 24 and 50 hours) using TiO_2 photoelectrodes and 100 mW/cm^2 from a solar simulator (ABET technologies, Sun 2000 Solar Simulators, USA) are shown in Fig. (4).
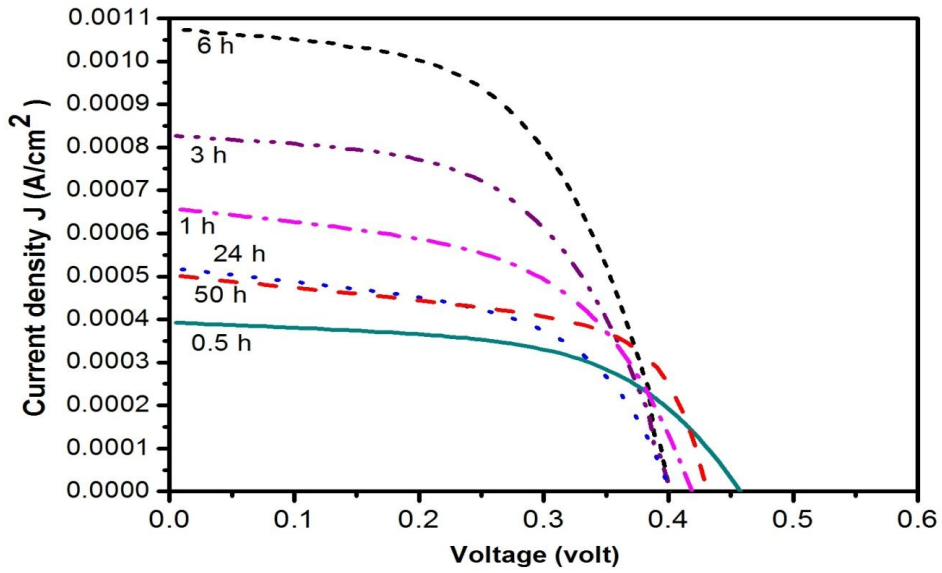
Fig. (4): J -V characteristics curves of a CdS$_{0.33}$Se$_{067}$ QDSSC for : 0.5,
1, 3, 6, 24 and 50 hours dipping time

Table (1): J -V characteristics parameters of CdS$_{0.33}$Se$_{067}$ QDSSCs for different
dipping times

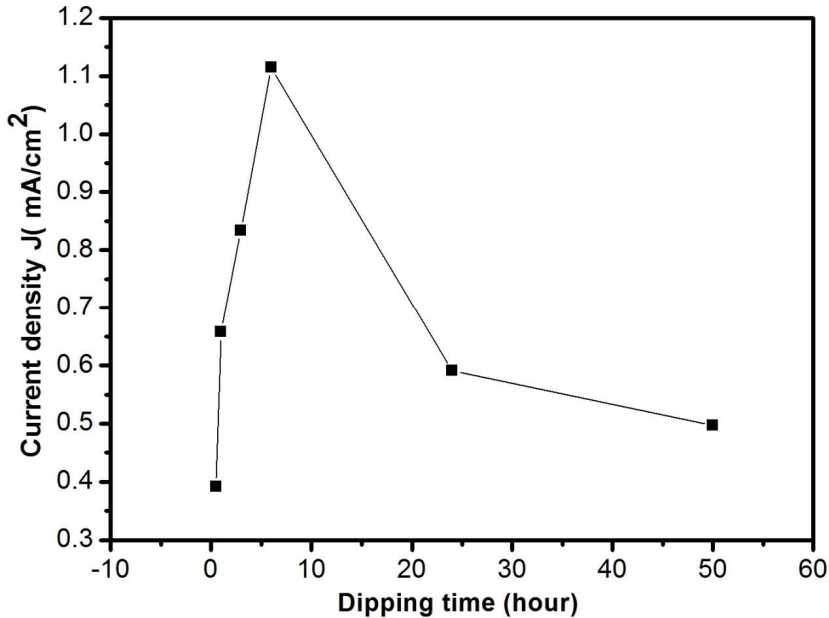| Dipping Time (hour)	V$_{oc}$ (mVolt)	J$_{sc}$ (mA/cm^2)	FF	η(%)
0.5	457	0.392	0.56	0.11
1	418	0.658	0.56	0.14
3	401	0.834	0.41	0.19
6	402	1.115	0.40	0.25
24	401	0.519	0.41	0.11
50	430	0.497	0.59	0.10

Fig. (5): Short current density of $CdS_{0.33}Se_{067}$ QDSSCs vs. Dipping Time.

Table, gives the measured values of V_{oc}, J_{sc}, fill factor (FF) and η for $CdS_{0.33}Se_{067}$ QDSSCs at different dipping times (0.5 -50 hr). It is clearly seen that in the dipping time range of 0.5–6 h, as dipping time the values of J_{sc} and η increase and approach maximum values (J_{sc} =1.115 mA/cm^{2}and and η = 0.25) at 6 h. Conversely, these values are lower (0.591 mA/cm^2 and 0.12%) and (0.497 mA/cm^2 and o.1 %) for dipping time 24 h and 50 h respectively. Fig. (5) shows the change in the case of J_{sc}. This can be explained as follows. According to the energetic alignments of CdS_xSe_{1-x} QDs and those of TiO_2 NPs, the conduction band $CdS_{0.33}Se_{067}$ QDs shifts closer to vacuum level as shown in Fig.6. The light from solar simulator generate electron hole pair (exciton) in alloyed CdS_xSe_{1-x} QDs. The electrons from the conduction band of the $CdS_{0.33}Se_{067}$ are quickly transferred to the conduction band of the TiO_2. Once the electrons diffuse into the conduction band of the TiO_2, the probability of its decay is small because there is no free hole in the TiO_2 under visible excitation. As a result, the electrons accumulate in the conduction band of the TiO_2 and the holes accumulate in the valance band of the CdS_xSe_{1-x} QDs. In this way, charge separation is achieved and hence generates photocurrent. It is necessary to employ a redox couple to scavenge the hole [33].
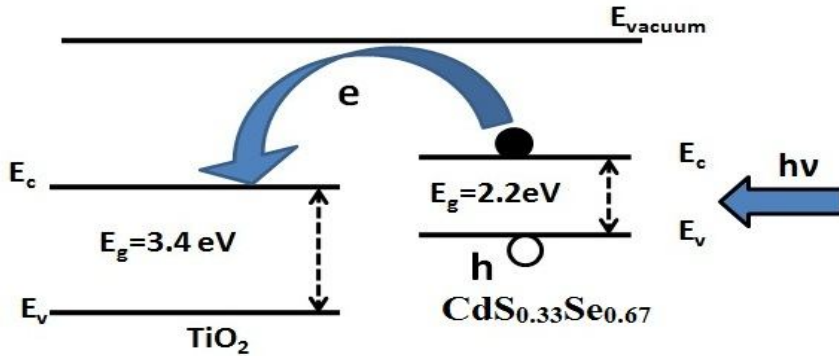
Fig. (6): Schematic diagram of charge transfer at TiO_2 $CdS_{0.33}Se_{067}$ QDs

However, as discussed above, the values of J_{sc} *and* η of the $CdS_{0.33}Se_{067}$ QDs/TiO_2 electrodes depend on the DA dipping time. Increasing the dipping time, the amount of QD loading will increase leading to an increase in the thickness of QDs cover the TiO_2 NP. Tran Chien Dang et al. [33] have made measurements on CdS /TiO_2 nanocomposite films and reported that, "only a thin slab having a suitable thickness around the interface between TiO_2 and CdS is contributing to the photocurrent current. Therefore, the maximum values of J_{sc} and η at 6 h dipping time support this argument. As the dipping time is increased more than 6 h, exciton generation by light absorption is larger, but the increase of thickness of $CdS_{0.33}Se_{067}$ QDs would take a longer time for the electrons to reach the interface. Therefore, the probability of recombination or trapping of the generated holes would be higher, causing the photocurrent to decrease. In contrast, for the $CdS_{0.33}Se_{067}$ QDs under 6 h dipping time, the decrease of the amount of QD loading will decrease the values of J_{sc} and η due to lower absorption of the CdS_xSe_{1-x} QDs films. Hence, the 6h DA dipping time seems to be a better candidate for a photovoltaic solar cell. Similarly, Prabakar et al. [14] have made measurements on J_{sc}, and η of CdS QDs onto TiO_2 NPs by CBD technique. In their work, they found that J_{sc} and η for 1 minute deposition time are better than those of higher dipping times. In our work, the long better dipping time (6 h) because, the DA process need long time to be optimized than CBD technique. The relatively long adsorption time in DA, helps in reducing the limiting effect of many parameters such as surface and solution cleanliness, QD concentration in the dispersion of TiO_2.

Figure (7) shows the performance of the assembled $CdS_{0.33}Se_{067}$ QDSSCs with various intensities of solar illumination (from 0 - 100% sun), the J-V characteristics curves were recorded for the 6 hours dipping time assembly. It is seen that as the intensity of the incident light increases, the measured J_{sc} increases linearly due to increased injected electrons.
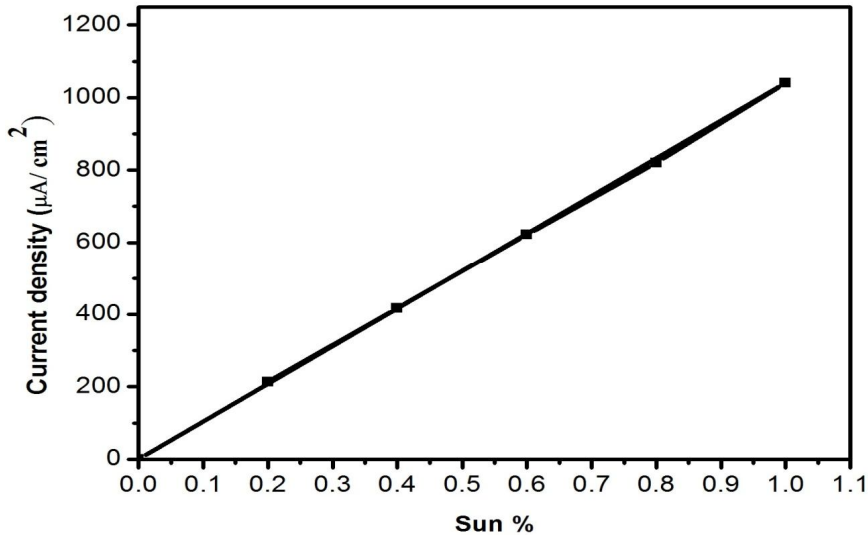
Fig. (7): Short circuit current J_{sc} vs. percentage of sun for a $CdS_{0.33}Se_{067}$ QDSSC for 6 hours dipping time

Conclusions :

QDs alloyed composite $CdS_{0.33}Se_{067}$ has been prepared using the chemical solution deposition technique. Vegard's law was applied to calculate the parameters of the EMA model. The calculated $CdS_{0.33}Se_{067}$ QDs size was found to be 3.1 nm, which is consistent with that determined using TEM. Alloyed $CdS_{0.33}Se_{067}$ were adsorbed onto TiO_2 NPs using the direct adsorption (DA) method, for different dipping times up to 50 h, as a sensitizer for photovoltaic cell. Our results show that the 6 h DA dipping time looks to be better for a photovoltaic solar cell. The reduction of both J_{sc} and η as the dipping time increases more than 6 are due to blocking the nanopores of TiO_2 layer by the additional amount of the loaded $CdS_{0.33}Se_{0.67}$ QDs. Furthermore, as the intensity of the incident solar light increases, J_{sc} increases linearly, indicating greater sensitivity of alloyed $CdS_{0.33}Se_{067}$ QDSSC.

Acknowledgments:

References:

1. Y.H. Lee, S.H. Im, J.H. Rhee, J.-H. Lee, S.I. Seok, *Applied Materials & Interfaces*, **2/6**, 1648 (2010).
2. A.J. Nozik, *Chemical Physics Letters*, 457, 3 (2008).
3. Y. Xie, S.H. Yoo, C. Chen, S.O. Cho, *Materials Science and Engineering*: B **177/1**, 106 (2012).
4. P. Yu, K. Zhu, A.G. Norman, S. Ferrere, A.J. Frank, A.J. Nozik, *J. Phys. Chem*. B **110**, 25451 (2006).
5. N. Guijarro, T. Lana-Villarreal, I. Mora-Sero´, J. Bisquert, R. Go´mez, J. Phys. Chem. C **113**, 4208 (2009).
6. J.H. Bang, P.V. Kamat, *ACS NANO*, **3**, 1467 (2009).
7. P. Sudhagar, J.H. Jung, S. Park, Y.-G. Lee, R. Sathyamoorthy, Y.S. Kang, H. Ahn, *Electrochemistry Communications*, 11, 2220 (2009).
8. K. Tvrdy, P.A. Frantsuzov, P.V. Kamat, *PNAS*, **108/1**, 29 (2011).
9. I. Barceló, T. Lana-Villarreal, R. Gómez, Journal of Photochemistry and Photobiology A: *Chemistry*, **220/1**, 47 (2011).
10. H. Chen, W. Li, H. Liu, L. Zhu, *Electrochemistry Communications*, **13/4**, 331 (2011).
11. X. Wang, H. Zhu, Y. Xu, H. Wang, Y. Tao, S. Hark, X. Xiao, Q. Li, *ACS NANO*, **4/6**, 3302 (2010).
12. W. Lee, S.K. Min, V. Dhas, S.B. Ogale, S.-H. Han, *Electrochemistry Communications*, **11**, 103 (2009).
13. T. Abdallah, K. Essawy, A. Khalid, S. Negm, H. Talaat, World Acaemy of Science, *Engineering and Technology*, **61**, 533 (2012).
14. K. Prabakar, H. Seo, M. Son, H. Kim, *Materials Chemistry and Physics*, **117**, 26 (2009).
15. A. Tubtimtae, M.-W. Lee, G.-J. Wang, *Journal of Power Sources*, **196/15**, 6603 (2011).
16. Y. Li, A. Pang, X. Zheng, M. Wei, *Electrochimica Acta*, **56/13**, 4902 (2011).
17. A. Tubtimtae, K.-L. Wu, H.-Y. Tung, M.-W. Lee, G.J. Wang, *Electrochemistry Communications*, **12**, 1158 (2010).
18. A. Kongkanand, K. Tvrdy, K. Takechi, M. Kuno, P.V. Kamat, *J. AM. CHEM. SOC*., **130**, 4007 (2008).
19. I.a. Mora-Ser´o, SixtoGim´enez, T. Moehl, F. Fabregat-Santiago, T. Lana-Villareal, R. G´omez, *J. Bisquert, Nanotechnology*, **19**, 424007 (2008).
20. S. Gim´enez, I.a. Mora-Ser´o, L. Macor, N. Guijarro, T. Lana-Villarreal, R. G´omez, L. J Diguna, Q. Shen, T. Toyoda, J. Bisquert, *Nanotechnology*, **20/29**, 295204 (2009).
21. D.R. Pernik, K. Tvrdy, J.G. Radich, P.V. Kamat, *J. Phys. Chem*. C 115/27 (2011).

22. A. Salant, M. Shalom, I. Hod, A. Faust, A. Zaban, U. Banin, *ACS NANO*, **4/10**, 5962 (2010).
23. P.V. Kamat, *J. Phys. Chem*. C **112/48**, 18737 (2008).
24. N.J. Smith, K.J. Emmett, S.J. Rosenthal, *Applied Physics Letters*, **93**, 043504 (2008).
25. D.V. Talapin, S. Haubold, A.L. Rogach, A. Kornowski, M. Haase, H. Weller, *J. Phys. Chem*. B **105/12**, 2260 (2001).
26. G. Syrrokostas, M. Giannouli, P. Yianoulis, *Renewable Energy*, **34**, 1759 (2009).
27. J.-H. Yum, S.-H. Choi, S.-S. Kim, D.-Y. Kim, Y.-E. Sung, *Journal of the Korean Electrochemical Society*, **10/4**, 257 (2007).
28. L. Brus, *J. Phys. Chem*., **90/12**, 2555 (1986).
29. M. Thambidurai, N. Murugan, N. Muthukumarasamy, S. Vasantha, R. Balasundaraprabhu, S. Agilan, *Chalcogenide Letters*, **6/4**, 171 (2009)
30. R. Sathyamoorthy, P. Sudhagar, R.S. Kumar, T.M. Sathyadevan, *Cryst. Res. Technol*., **45/1**, 99 (2010).
31. L.A. Swafford, L.A. Weigand, M.J. Bowers, J.R. McBride, J.L. Rapaport, T.L. Watt, S.K. Dixit, L.C. Feldman, S.J. Rosenthal, *J. Am. Chem. Soc*. **128**, 12299 (2006).
32. O. Madelung, Semiconductors : Data Handbook, Springer-Verlag, Berlin, (2004).
33. T.C. Dang, D.L. Pham, H.C. Le, V.H. Pham, Adv. Nat. Sci.: Nanosci. Nanotechnol. 1 (2010) 015002 (5pp).